American Mineralogist, Volume 84, pages 871–876, 1999

Formation of rutile nuclei at anatase {112} twin interfaces and the phase transformation mechanism in nanocrystalline titania

R. LEE PENN[1,*] AND JILLIAN F. BANFIELD[2]

[1]Materials Science Program, University of Wisconsin, Madison, Wisconsin 53706, U.S.A.
[2]Department of Geology and Geophysics, University of Wisconsin, Madison, Wisconsin 53706, U.S.A.

ABSTRACT

In nanocrystalline anatase coarsened under hydrothermal conditions (250 °C, P_{sat}), the anatase-to-rutile phase transformation is nucleated at anatase {112} twin boundaries formed by oriented attachment. The anatase twin boundary is constructed from structural elements common to rutile. Specifically, rutile nucleation involves displacement of only one half the titanium cations within the twin slab. Subsequent transformation of bulk anatase involves rupture of 7 of the 24 Ti-O bonds per unit cell and cooperative displacement of Ti and O. As the transformation advances into the bulk material, adjacent slabs of anatase octahedra are destabilized, resulting in rapid progression of the transformation of bulk anatase to rutile. The implied chain reaction, scarcity of partly reacted crystals, absence of multiply twinned rutile, and the importance of nucleation at anatase twins indicate a rate law based on slow nucleation and rapid growth. The displacements are comparable to those proposed previously for macroscopic anatase at much higher temperatures, indicating the atomic mechanism is not modified by particle size or temperature, despite the rapid kinetics in finely crystalline aggregates. In addition to the formation of twins, clusters with rutile-like character may occur at some fraction of random anatase-anatase particle contacts. Such interfaces should result in decreased activation barriers for rutile nucleation and, thus, contribute significantly to the observed faster transformation rates in nanocrystalline compared to coarsely crystalline materials.

INTRODUCTION

TiO_2 occurs in at least seven different polymorphic forms, four of which are found in nature. Rutile is a crystallization product of igneous rocks, and rutile, anatase, brookite, and TiO_2(B) occur as accessory minerals in alteration assemblages and sedimentary and metamorphic rocks (Banfield et al. 1991; Banfield and Veblen 1991 and 1992). Anatase is typically the majority product of inorganic syntheses and is the main constituent of nanocrystalline materials developed as catalytic supports and gas phase separation membranes.

Most prior analyses imply that rutile is the stable phase at all temperatures up to the melting point and all pressures up to several tens of kilobars. However, the structure energy of anatase is close to that of rutile (Post and Burnham 1986). Based on the inferred lower surface energy of nanocrystalline anatase, phase stability reversal is predicted at particle sizes of <13 nm (Gribb and Banfield 1997; Zhang and Banfield 1999), and supported by coarsening and phase transformation experiments (Gribb and Banfield 1997). Thus, the kinetics of the anatase-to-rutile phase transformation are dependent on anatase crystal size, as well as temperature, pressure, fluid abundance, and chemistry.

*Current address: The Johns Hopkins University, Department of Earth and Planetary Sciences, Olin Hall, Baltimore, MD 21218, U.S.A. E-mail: leepenn@jhunix.hcf.jhu.edu

Anatase and rutile are constructed from octahedrally coordinated Ti cations arranged in edge sharing chains, as shown in Figure 1. Octahedra in anatase share four edges and are arranged in zigzag chains parallel to [221]. Rutile Ti octahedra share only two edges and form chains along [001]. The reaction of bulk anatase to rutile requires rotation of half the Ti octahedra.

Banfield and Veblen (1992) analyzed structural relationships between the TiO_2 polymorphs that may have significance for phase transformation mechanisms. They noted a polytypic rather than polymorphic relationship between brookite and anatase and the absence of extensive structural units common to anatase and rutile. This approach did not consider the potential importance of twinning. Penn and Banfield (1998) showed that anatase {112} twins, formed by oriented attachment, can be defined as one unit cell of brookite and that atomic displacements contained within the twin interface may nucleate a phase transformation between anatase and brookite. Banfield and Veblen (1992) also noted that brookite and rutile have common structural slabs containing octahedra that tilt in alternating directions. The {112} anatase twin interface also has a structural similarity to rutile; as shown in Figure 1, the twin interface consists of two slabs of octahedra arranged in zigzag chains. In rutile, the chains are linearly disposed throughout the structure. Half of the octahedra in this two-octahedra-thick slice of anatase are common to rutile (Fig. 1) and the other half are not. This paper shows that this twin surface can serve to nucleate the anatase-to-rutile phase transformation.

0003-004X/99/0506–0871$05.00

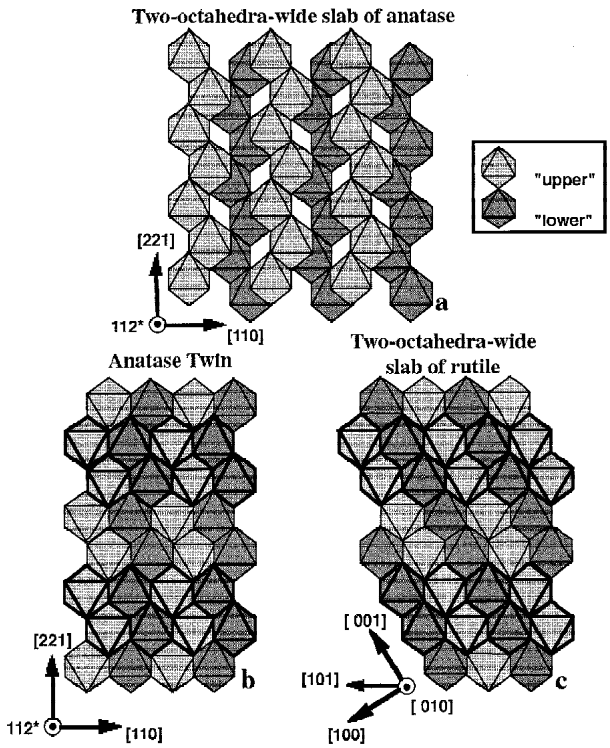

FIGURE 1. Anatase **(top)**, anatase {112} twin **(right)**, and rutile **(left)**. Bold-outlined octahedra highlight the strips common to the anatase twin and rutile structures.

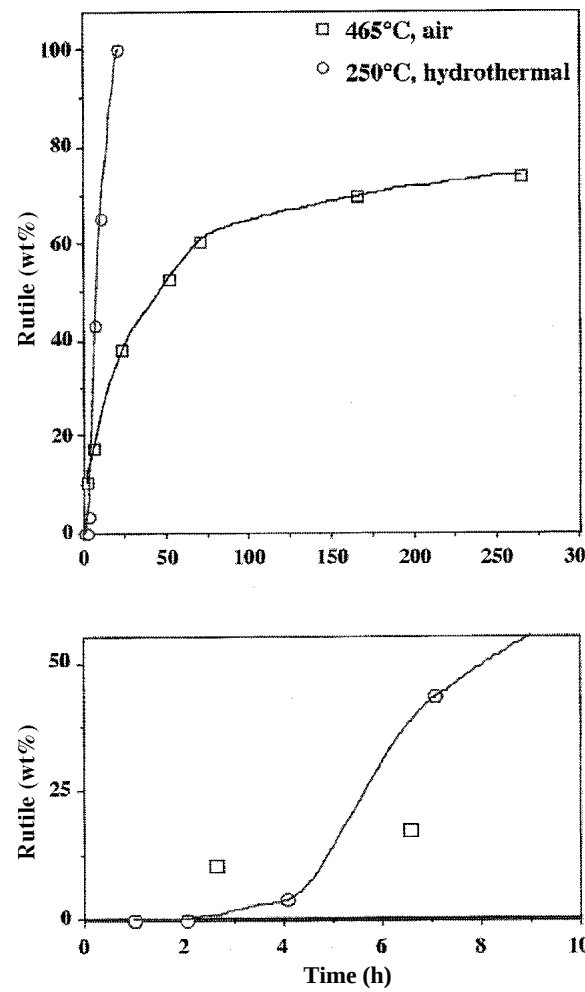

FIGURE 2. (top) Rutile content as a function of treatment time. The data for titania coarsened in air at 465 °C, open squares data from Gribb and Banfield (1997). Open circles tiitania suspensions (0.13 *M* HCl [$-\log(a_{H+})$ = 1.2 at 250 °C and P_{sat}, 3 mg titania per 1 mL suspension] were hydrothermally coarsened. **(bottom)** Magnification of the first 10 h of treatment. Note the delay in rutile formation in the hydrothermally coarsened samples.

Previous coarsening data showed a significant increase in the anatase to rutile transformation rate with decreased particle size (Suzuki and Tukuda 1969; Banfield et al. 1993; Kumar et al. 1993; Gribb and Banfield 1997). This study shows that under hydrothermal conditions, the growth and phase transformation rates are significantly enhanced in comparison to coarsening experiments involving similar nanocrystalline materials performed in air. The implications of the kinetics of a twin-mediated phase transformation are discussed.

EXPERIMENTAL METHODS

Nanocrystalline anatase (~5 nm in diameter) was synthesized via the sol gel method (Bischoff 1992; Gribb and Banfield 1997). Following synthesis, anatase suspensions were dialyzed using a Spectra/Por (MWCO = 2000) membrane in DI water (changed 11 times) to remove the byproducts of synthesis. Prior to dialysis, suspensions of anatase had not gelled and had low viscosity (similar to that of water). Following dialysis, the suspensions had gelled and were highly viscous, indicating that the pH had risen to near the isoelectric point of anatase (measured pH ~5.5). This coincides with the isoelectric point range reported by Bischoff (1992). XRD characterization shows the starting material to consist of 94% anatase and 6% brookite (Penn and Banfield 1998).

Suspensions (~3 mg anatase per 1 g solution) in the Teflon cups of Parr Instrument Company's 4744 general purpose acid digestion vessels were placed into a furnace held at temperatures ranging from 100 to 250 °C for times ranging from 1 h to 255 h. Vessels were removed and allowed to cool to room temperature. The H+ activities at hydrothermal conditions were estimated based on room temperature pH measurements using Soluble, a FORTRAN program that calculates speciation (Roselle and Baumgartner 1995). Equilibrium constants for hydrochloric acid were taken from Sverjensky et al. (1991).

Hydrothermally treated suspensions were diluted, and one drop of diluted solution was placed onto a Formvar-coated copper grid for examination using the Philips CM200 200 kV HRTEM with a Cs ~0.5 mm.

Several drops of undiluted solution were placed on a low background sample holder for XRD analysis using the Scintag Pad V 4-axis X-ray diffractometer. Particle size was determined from peak broadening using the Scherrer equation. Average particle dimensions were verified by measurements from micrographs. Particle sizes were measured along <101> and [001].

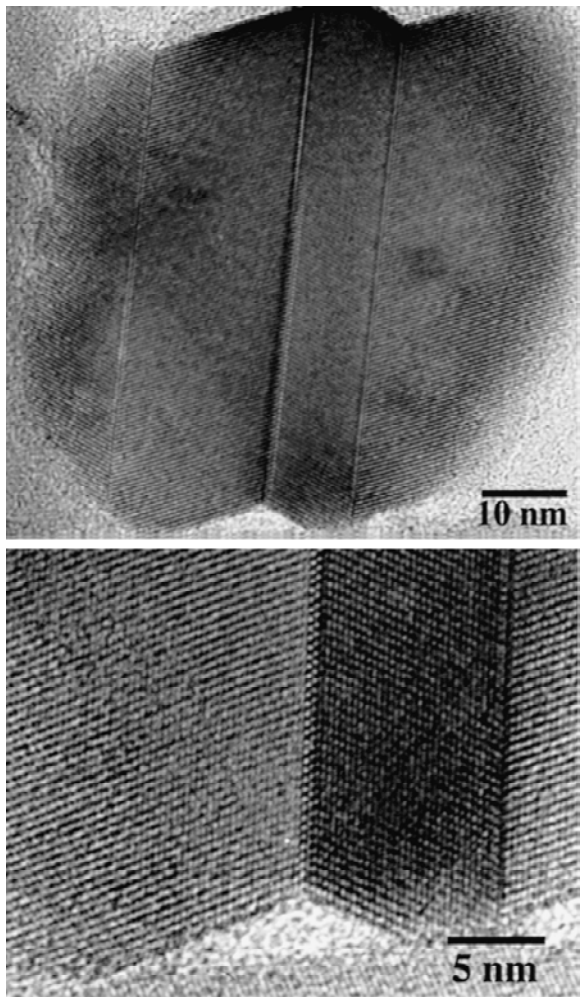

FIGURE 3. HRTEM micrograph of a twinned anatase particle viewed down <131>.

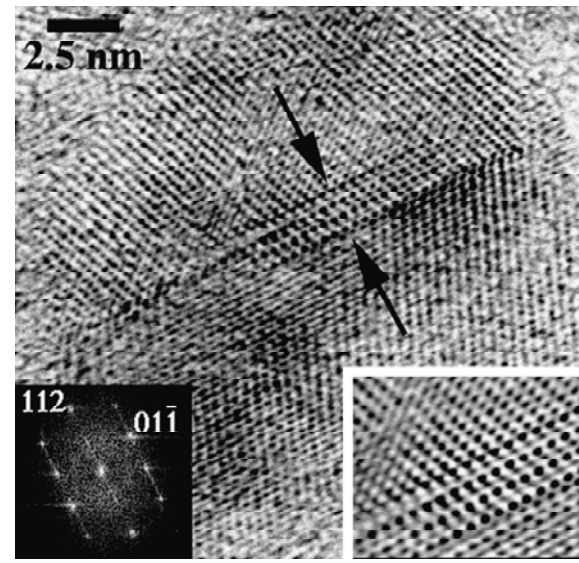

FIGURE 4. Rutile nuclei (indicated by arrows) on the {112} anatase twin surface (viewed down [131] anatase). Inset (lower right) shows rotationally filtered interface.

Anatase/rutile/brookite content was estimated by comparison of relative X-ray diffraction intensities of the anatase (101), rutile (110), and brookite (121) peaks. The rutile content in each sample was determined following the standardization used by Gribb and Banfield (1997).

RESULTS

Figure 2 shows the rutile content as a function of time for a suspension of starting material, 0.13 *M* HCl [$-\log(a_{H^+}) = 1.2$ at 250 °C and P_{sat}] and 3 mg titania per mL suspension, hydrothermally treated at 250 °C and P_{sat}. The minimum average particle size measured for the first appearance of rutile (<1 wt% rutile) using X-ray diffraction was approximately 40 nm (using peak broadening analysis). Variation of the conditions of hydrothermal treatment (acid type and concentration) did not change this initial average rutile size. HRTEM data show the as-synthesized anatase to be free of dislocations and intergrowths. Rutile crystals formed by phase transformation from anatase are frequently twinned on (010), but are free of other intergrowths. Specifically, no complex rutile twins (meaning more than two twin-related crystals) were observed.

Figure 3 shows a particle from a sample hydrothermally treated at 250 °C for 262 h. This sample consists of 60 wt% rutile and 40 wt% anatase (trace of brookite). This twinned particle consists of four slabs of anatase viewed down the <131>. The vertical twin plane between the anatase crystals is {112}.

Figure 4 shows a twinned anatase with slabs of a different material adjacent to the {112} anatase twin surface. This sample was hydrothermally treated for 71.8 h at 250 °C and was 12% rutile, 2% brookite, and 86% anatase. The slab is four layers thick and is clearly distinct from a slab of brookite, as verified by comparisons to both image simulations and HRTEM images of brookite in relevant orientations (as described by Penn and Banfield 1998). Based on the periodicity parallel to the twin plane, XRD results, and image details, we infer that this is a four-unit-cell-wide rutile nuclei. If so, it is the first observation of an anatase nanocrystal partially transformed to rutile. All other observations are of particles comprised solely of anatase, anatase and brookite (see Penn and Banfield 1998), or rutile. If the material at the interface is rutile, the rutile (010) planes are parallel to the anatase {112} planes.

The angular relationship to either side of the twin interface of a rutile particle viewed down [111] is nearly identical to the angular relationship between twin-related anatase (Fig. 5). The twin interface is rutile {010}. The crystal morphology is dominated by the {110} faces, as expected by the Donnay-Harker rules (Donnay and Harker 1937), which relate surface energy to *d*-values.

DISCUSSION

We have shown that anatase {112} twins form via oriented attachment (Penn and Banfield 1998). Here, we show that these twins are the key to the nucleation of the anatase-to-rutile phase

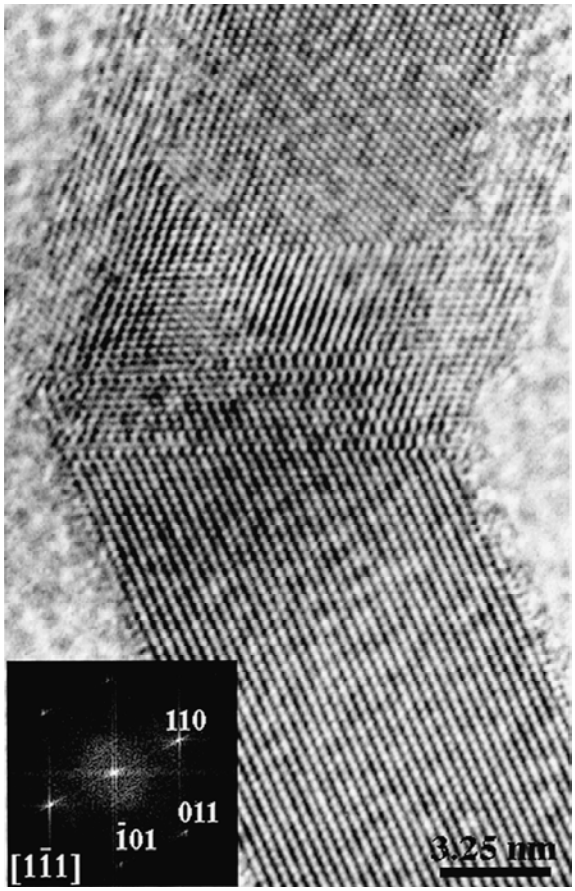

FIGURE 5. HRTEM image of rutile, viewed down [111]. This rutile particle has preserved the parent anatase twin morphology. Rutile {110} planes, the lowest surface energy planes, bound the product crystal.

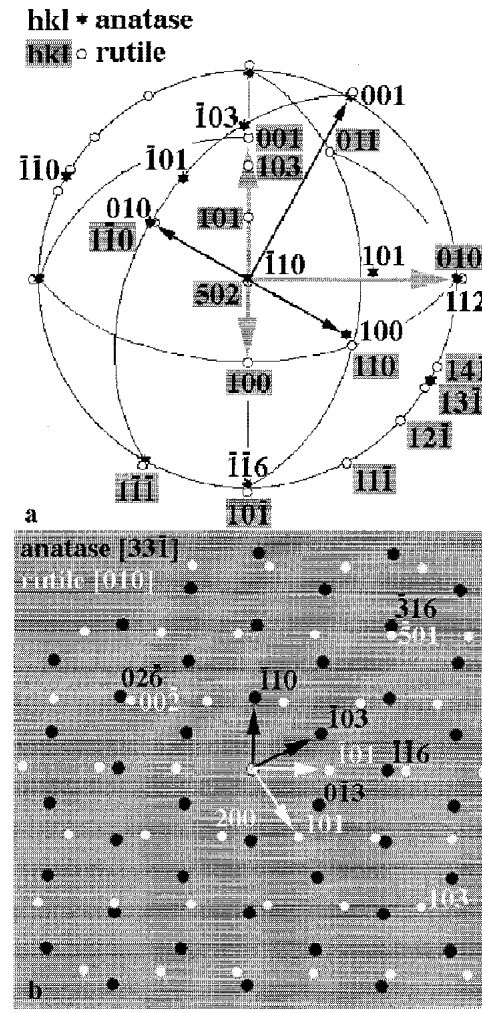

FIGURE 6. (a) Steronet showing the relationships between the reciprocal lattices of anatase and rutile. **(b)** Diagram illustrating the superimposition of reciprocal lattice points within the plane of the anatase-rutile interface (i.e., viewed down anatase 112*).

transformation. Given that rutile particles retain the parent anatase twin morphology, the crystallographic relationship between the polymorphs is proposed by inferring the pre-transformation orientation of anatase in Figure 5 from the morphology seen in Figure 4. Detailed examination of the anatase and rutile structures show that the oxygen closest packed planes, (010) for rutile and {112} for anatase, are parallel and [010] in anatase is parallel to [$1\bar{0}1$] in rutile. This result is consistent with the relative orientations of anatase and rutile inferred from Figures 4 and 5, and reveals the atomic displacements necessary for the anatase to rutile phase transformation.

Figure 6 shows the relationship between the structure of the anatase {112} twin interface and the structure of rutile viewed down [110] anatase, with the respective orientations constrained by the crystallographic relationships shown in Figure 7. Both have strips of Ti octahedra in common. Adjacent strips are stacked along [221] in anatase but are displaced by one octahedron along [101] in rutile (Figs. 1 and 6). Transformation of the twin interface into a slab of rutile involves inheritance of one half the Ti octahedra and requires displacement of the other half of the Ti. In Figure 1, this occurs in the strips of material comprising the twin interface that are not common to both structures. Displacements are 2.7 Å along anatase [110].

It should be noted that two {112} interface structures are possible, one of which is the twin described above. The other involves face-sharing octahedra. However, this arrangement is predicted to be unlikely as face sharing between Ti octahedra is energetically unfavorable. Furthermore, evidence for the existence of interfaces characterized by face sharing was not found.

The transformation propagates from rutile formed at twin surfaces into the surrounding anatase (Fig. 8). The reaction involves cooperative displacements of O anions and Ti cations and requires four different sets of Ti displacements within slabs of {112} anatase octahedra (Table 1). The transformation can be viewed as a displacement of Ti and O planes. As the transformation progresses, the O plane adjacent to the Ti cation plane comprising the leading edge of the transformation is distorted. The next plane of ions, Ti cations, are all displaced by approximately 1.8 Å along ~<331>. The transformation continues, with

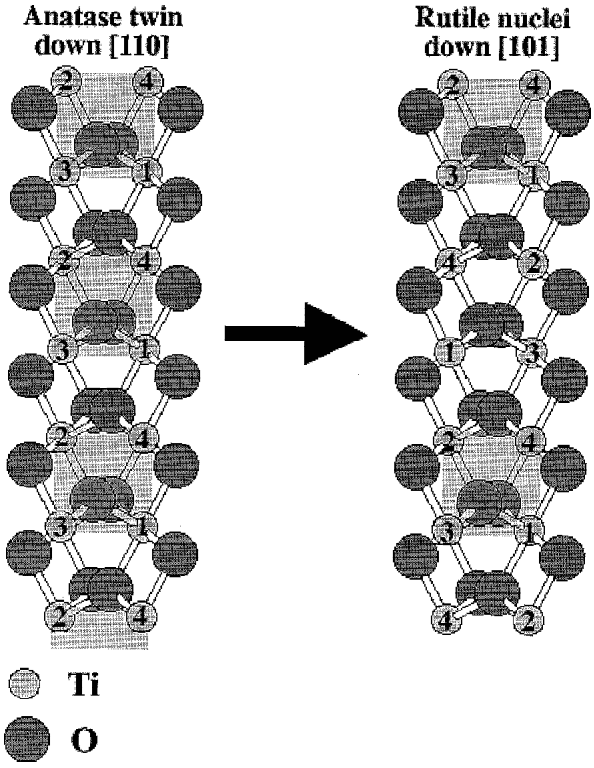

FIGURE 7. Schematic representation of rutile nucleation event: octahedral slabs to either side of the anatase {112} twin boundary. Shaded boxes indicate octahedra inherited in the transformed material. Numbers indicate height (in units of 1.34 Å) along [110]. Displacement of Ti cations, those octahedra not included in the shaded boxes, required to transform these planes to rutile is 2.7 Å parallel to anatase <110>.

displacements of the next O plane by ~1.4 Å along <221>, the next Ti plane by 1.3 Å along <110>, the next O plane by 1.4 Å along <221>, and the next Ti plane by 1.8 Å along ~<$\bar{3}3\bar{1}$>. At this point, the mechanism repeats, so one half of the Ti octahedra are inherited in the next slab transformed. Every fourth (112) cation plane involves two-octahedra-wide strips common to rutile that alternate with two-octahedra-wide strips not common to rutile.

The displacements (Table 1, Fig. 8) are systematically related to those proposed for the brookite-to-rutile transformation (Barblan et al. 1958). This result is expected, given the polytypic relationship between anatase and brookite (Banfield and Veblen 1992; Penn and Banfield 1998).

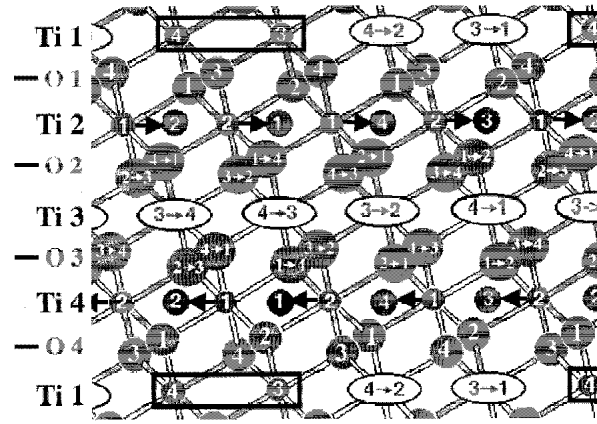

FIGURE 8. Proposed mechanism for the anatase → rutile transformation. Ti (small circles and white ovals) and O (large grey circles). Numbers designate the location of cations and O in four levels along the projection direction (anatase [110]). Arrows indicate displacements left to right and between cation and O levels.

The mechanism of the transformation of nanocrystalline anatase under hydrothermal conditions at 250 °C bears strong similarity to the mechanism proposed by Shanon and Pask (1964) for single crystals of millimeter dimensions at 900–950 °C. Specifically, the majority of the ion displacements are contained within the anatase {112} planes. This result is important because it is the first verification that the mechanism is constant over a several hundred degrees Celsius temperature range and is not modified by the high surface area to volume ratio of the nanocrystalline material, despite the greatly accelerated reaction rate for small particles.

We infer that the anatase-to-rutile phase transformation in nanocrystalline materials is rate limited by rutile nucleation, as opposed to rutile growth. This is supported by the scarcity of partly reacted crystals, implying that complete conversion rapidly follows rutile nucleation (Gribb and Banfield 1997). Absence of rutile nuclei in anatase coarsened hydrothermally, except at anatase twin planes (Fig. 4), suggests the lower activation barrier for rutile crystallization at these sites has an important kinetic effect. In addition, the large average particle size of the first detected rutile implies rapid rutile growth and possible significant overstepping of the (size-dependent; Banfield et al. 1993; Kumar et al. 1993; Gribb and Banfield 1997) anatase-rutile phase boundary.

TABLE 1. Estimates for displacement vectors in each plane of Ti and O

Atom	Displacements	Bonds broken
Ti	1/2 inherited	0
	1/2 displaced (2.7 Å || <110>)	8
O	distortions	
Ti	all displaced (1.2 Å || <111> + 1.3 Å || <110>) = 1.8Å ||~<331>	8
O	all displaced (1/2 Å || <111> + 1.3 Å || <110>) = 1.4 Å ||~<221>	
Ti	all displaced (1.3 Å || <110>)	4
O	all displaced (1/2 Å || <111> + 1.3 Å || <110>) = 1.4 Å ||~<221>	
Ti	all displaced (-1.2 Å || <111> + 1.3 Å || <110>) = 1.8Å || ~<$\bar{3}3\bar{1}$>	8
		Total = 28 / 96

Rutile particles are typically singly twinned on (010) or exist as homogeneous single crystals. Shannon and Pask (1964) predicted four orientations of rutile due to the fourfold symmetry of the reactant anatase. However, complex twinning (excluding the simple twins inherited from anatase) or symmetry-related intergrowths are not observed in rutile particles in this study, suggesting that nucleation typically occurs at a single site within each transforming particle. This is interpreted as further evidence that rutile nucleation in anatase, rather than rutile growth, is the rate limiting step in anatase-to-rutile phase transformation.

Phase transformation rates can be size dependent (Banfield et al. 1993; Kumar et al. 1993; Gribb and Banfield 1997). Gribb and Banfield (1997) analyzed possible explanations for this phenomenon in nanocrystalline anatase, and concluded the effect probably occurs through the nucleation term. For hydrothermally coarsened anatase, results reported here suggest this specifically involves lowering of the activation energy due to introduction of rutile-like features at twin planes. If oriented attachment is shown to be a common coarsening and microstructure-producing mechanism in natural and synthetic materials, similar effects on phase transformation kinetics may be found in other systems.

Although the driving forces for oriented attachment are high (Averback et al. 1996), some reactions will occur under conditions where particle rotation is restricted (e.g., the kinetic experiments of Gribb and Banfield 1997, where water was essentially eliminated by pretreatment). However, in these cases, less crystallographically specific particle-particle contacts may also contribute to nucleation of rutile where contacts coincidentally introduce smaller clusters with rutile-like character. This may partly explain the approximately linear dependence of coarsening and phase transformation rates in nanocrystalline titania aggregates (Gribb and Banfield 1997).

ACKNOWLEDGMENTS

The authors would like to acknowledge financial support from the National Science Foundation (Grant No. EAR-9508171), the National Physical Science Consortium (fellowship to R.L.P. sponsored by Sandia National Laboratories), and the Mineralogical Society of America for a student research grant to R.L.P. We wish to express thanks to Hengzhong Zhang for helpful insights and comments. This manuscript was greatly improved by the careful reviews and editorial comments of P. Buseck, M. O'Keefe, and L. Bursill.

REFERENCES CITED

Averback, R.S., Zhu, H., Tao, R., and Höfler, H. (1996) Sintering of nanocrystalline materials: experiments and computer simulations. In D.L. Bourell, Ed., From Synthesis and Processing of Nanocrystalline Powder, p. 203–216. The Minerals, Metals, and Materials Society, Warrendale, Pennsylvania.

Banfield, J.F. and Veblen, D.R. (1991) The structure and origin of Fe-bearing platelets in metamorphic rutile. American Mineralogist, 76, 113–127.

—— (1992) Conversion of perovskite to anatase and TiO_2 (B): A TEM study and the use of fundamental building blocks for understanding relationships among the TiO_2 minerals. American Mineralogist, 77, 545–557.

Banfield, J.F., Veblen, D.R., and Smith, D.J. (1991) The identification of naturally occurring TiO_2 (B) by structure determination using high-resolution electron microscopy, image simulation, and distance-least-squares refinement. American Mineralogist, 76, 343–353.

Banfield, J.F., Bischoff, B.L., and Anderson, M.A. (1993) TiO_2 accessory minerals: coarsening, and transformation kinetics in pure and doped synthetic nanocrystalline materials. Chemical Geology, 110, 211–231.

Barblan, F., Brandenberger, E., and Niggli, P. (1958) Geregelte und ungeregelte strukturen von titanaten und ferriten und geregelte umwandlungen der TiO_2-Modifikationen. Helvetica Chimica Acta, 27, 88–96.

Bischoff, B.L. (1992) Thermal stabilization of anatase membranes. Ph.D. Thesis, University of Wisconsin, Madison, Wisconsin.

Donnay, J.D. and Harker, D. (1937) A new law of crystal morphology extending the law of Bravais. American Mineralogist, 22, 446–467.

Gribb, A.A. and Banfield, J.F. (1997) Particle size effects on transformation kinetics and phase stability in nanocrystalline TiO_2. American Mineralogist, 82, 717–728.

Kumar, K.P., Keizer, K., and Burggraaf, A.J. (1993) Textural stability of titania-alumina composite membranes. Journal of Materials Chemistry, 3, 917–922.

Penn, R.L. and Banfield, J.F. (1998) Oriented attachment and growth, twinning, polytypism, and formation of metastable phases: insights from nanocrystalline TiO_2. American Mineralogist, 83, 1077–1082.

Post, J.E. and Burnham, C.W. (1986) Ionic modeling of mineral structures and energies in the electron gas appropximation: TiO_2 polymorphs, quartz, forsterite, diopside. American Mineralogist, 71, 1142–1150.

Roselle, G. and Baumgartner, L. (1995) Experimental determination of anorthite solubility and calcium speciation in supercritical chloride solutions at 2kbar from 400 to 600 °C. Geochimica et Cosmochimica Acta, 59, 1539–1549.

Shanon, R.D. and Pask, J.A. (1964) Topotaxy in the anatase-rutile transformation. American Mineralogist, 49, 1707–1717.

Suzuki, A. and Tukuda, R. (1969) Kinetics of the transition of titanium dioxide prepared by sulfate process and chloride process. Bulletin of the Chemical Society of Japan, 42, 1853–1857.

Sverjensky, D.A., Hemley, J.J., and D'Angelo, W.M. (1991) Thermodynamic assessment of hydrothermal alkali feldspar-mica-aluminosilicate equilibria. Geochimica et Cosmochimica Acta, 55, 989–1004.

Zhang, H. and Banfield, J.F. (1998) Phase stability in the nanocrystalline TiO_2 system. In E. Ma, P. Bellon, M. Atzmon, R. Trivedi, MRS, Eds., Phase Transformations and Systems Driven Far From Equilibrium. Materials Research Society Proceedings, 481, 619–624. Warrendale, Pennsylvania.

MANUSCRIPT RECEIVED JUNE 9, 1998
MANUSCRIPT ACCEPTED DECEMBER 5, 1998
PAPER HANDLED BY PETER R. BUSECK